^{3}He-induced fission of nuclei $159 < A < 232$

F. D. Becchetti

Department of Physics, University of Michigan, Ann Arbor, Michigan 48109

K. H. Hicks, C. A. Fields, R. J. Peterson, R. S. Raymond, R. A. Ristinen, J. L. Ullmann, and C. S. Zaidins

Nuclear Physics Laboratory, Department of Physics, University of Colorado, Boulder, Colorado 80309

(Received 4 May 1983)

The fission of nuclei with $159 \leq A \leq 232$ induced by the bombardment of 19.1 to 44.5 MeV ^{3}He ions has been measured using solid-state detectors with time-of-flight measurements. Analysis with statistical fission theory, including precompound nucleon emission, indicates fission barriers which decrease only slightly relative to the liquid-drop model values with decreasing Z, approaching about 90% of the liquid-drop model barrier for $A \approx 160$. These results are in contrast with measurements at higher angular momenta which indicate much lower fission barriers (60 to 70 % of the liquid-drop model) for this mass region. The angular correlations indicate complete, or slightly greater than complete momentum transfer to the compound system. This is in opposition to that observed using heavier projectiles where incomplete momentum transfer is probable.

I. INTRODUCTION

The liquid-drop model[1] (LDM) is the basis for our understanding of many nuclear properties: masses, binding energies, and decay phenomena such as spontaneous fission.[2,3] The stability of nuclei with $A > 150$ is generally determined[4] by the competition between β decay, α decay, spontaneous fission (SF), and, perhaps, decay of the nucleon. The β-stable nuclei, $A > 150$, which are thought of as "stable," can nonetheless decay via α emission and SF albeit with very long half-lives,[4,5] e.g., $T_{1/2} = 10^{10}$ to $> 10^{130}$ years. The calculated SF rates for these nuclei, as well as those for superheavy elements ($A \approx 300$) are sensitive to the LDM fission barrier.

Recently, several analyses of reaction-induced fission using heavy ions ($A > 4$) (Refs. 6—9) and very energetic light ions[10-12] have indicated rather low fission barriers (60 to 70% of the LDM value) particularly for nuclei with $A < 190$. Heavy ions and energetic light ions deposit large amounts of energy, mass, and most important, angular momentum. The latter greatly affects the fission process[2,3] and extraction of an LDM fission barrier in the presence of about one hundred units of angular momentum is *highly* model dependent.[13]

The problem of excessive angular momentum, mass, and energy transfer can be minimized by the use of light projectiles at relatively low bombarding energies. Although the fission probability for nuclei $A < 190$ is then quite small,[14] the process is more adiabatic and amenable to theoretical interpretation. Also, light-ion induced fission involves nuclei near the line of beta stability where nuclear properties, e.g., level densities are best known.

Although many data exist for light-ion induced fission,[2,3] these are concentrated near $A = 230$ and most of the data[15-18] available for lighter elements ($A < 210$) have been obtained by radiochemical methods, fission track detectors, or first-generation solid state detectors without good time-of-flight measurements. These methods did not always offer good discrimination against trace heavy impurities or yield accurate mass-energy data.

In the present paper we present the bombarding-energy and target-mass dependence of fission cross sections determined with 19.1 to 44.5 MeV ^{3}He beams using solid-state detectors in coincidence for fragment energy and time of flight. A more complete analysis of the angular correlations and angular distributions will be presented in subsequent work.

II. EXPERIMENT

A. Beam

A variable energy ^{3}He beam from the University of Colorado sector-focused cyclotron, focused to a 3×3 mm spot ($\delta\theta < 0.5°$) was used to bombard targets placed in a 1 m diameter scattering chamber. The beam pulse was 1 to 2 ns wide on the target. The time structure of the beam was monitored by observing γ rays from the beam stop which was located approximately 1 m downstream from the chamber.

B. Detectors

Coincident (and noncoincident) fission fragments were detected with 300 or 600 mm^2 silicon surface-barrier

detectors, 60 to 150 μm thick, placed on opposing movable arms. Secondary target electrons were suppressed by magnets. The target-detector distances were typically 15 to 40 cm and the solid angles of the detectors were 1.2 to 20 msr, corresponding to angular acceptances of 2° to 8°.

The signals from the detectors were input to charge-sensitive preamps which produced fragment energy and fast timing signals. The latter were combined to produce spectra of the fragments' time of flight, both relative to the cyclotron beam burst and between pairs of opposing detectors. The energy and timing signals were event-mode recorded with an on-line computer.

Energy and timing calibrations were obtained using α sources and a thin ^{252}Cf spontaneous-fission source. The energy and timing relative to the beam pulse were checked by observing ^{12}C recoils from a thin carbon target in coincidence with scattered ^{3}He ions. The pulse-height defects of the detectors[22] were determined by comparisons of the apparent α and ^{252}Cf fragment energies to accepted values. The short-term time resolution was 0.7 to 1 ns (FWHM) while the long-term time resolution was 1.0 to 1.5 ns.

The relative angle settings between the detector arms were checked optically and by measuring the ^{252}Cf fission-fragment angular correlation ($\theta_1 - \theta_2 = 180°$). The relative angle readings were typically within $\pm 0.1°$ of the true values. In addition, the incident angle and position of the ^{3}He beam on the target were limited by a set of entrance collimators to $\pm 0.3°$ and ± 3 mm, respectively. Angular correlation measurements ($\theta_1 - \theta_2$) were also done as a function of the target rotation angle, the detector-target distance, and target axis position. Data taken with small detector-target distances showed variations in $\theta_1 - \theta_2$ of 1° to 3° and were subsequently renormalized, as needed, to the data taken at larger detector-target settings. The overall accuracy of the angular correlations ($\theta_1 - \theta_2$) was checked by observing coincident ^{12}C and ^{3}He recoils from a carbon target. It was found to be consistent with the combined accuracy of the beam geometry and detector arm settings, namely, $< \pm 0.5°$.

The targets and beam were monitored using a solid-state detector placed at $\theta = 28° \pm 0.5°$ and set to observe ^{3}He elastic scattering. In a few cases the monitor was also used to check or infer target thicknesses.

C. Targets

Most of the targets consisted of self-supporting rolled metal, 500 to ≥ 600 μg/cm^2 thick, or material evaporated onto thin carbon or Al backings. A few thick targets of thicknesses > 1 mg/cm^2 were also employed. The targets investigated are listed in Table I.

Heavy contaminants in the targets usually could be identified in the fission-fragment spectra from the summed fragment energy spectra (see Sec. III C). Targets of questionable purity were subsequently checked with x-ray fluorescence, which can indicate the presence of high-Z impurities, typically Ta, Pb, Th, or U, with a sensitivity better than one part in 10^4. Data from targets exhibiting large contaminations (e.g., Lu) were not used.

TABLE I. Targets.

Element	Isotopic[a] enrichment (%)	ρx[b] (mg/cm^2)	Type	Backing
$_{65}$Tb (nat)	159(100)	0.50	Self-supporting rolled[c]	None
$_{67}$Ho (nat)	165(100)	0.48	Self-supporting rolled[c]	None
$_{69}$Tm (nat)	169(100)	0.52	Self-supporting rolled[c]	None
$_{71}$Lu (nat)	175(97.4) 176(3.6)	0.53	Self-supporting rolled[c]	None
$_{73}$Ta (nat)	181(99.9)	0.60	Evaporated	0.2 mg/cm^2 Al
$_{75}$Re (nat)	185(37.5) 187(62.5)	1.58	Evaporated	0.4 mg/cm^2 Al
$_{78}$Pt	194($>$90)	0.16	Evaporated	0.02 mg/cm^2 C
	195(97.3)	0.60	Self-supporting rolled[c]	None
$_{79}$Au (nat)	197(100)	0.21	Self-supporting rolled[c]	None
		0.90	Self-supporting rolled[c]	None
$_{80}$Hg	202($>$90)	2.75	Evaporated	0.5 mg/cm^2 Mg
$_{81}$Tl	205(99.9)	0.20	Evaporated	0.04 mg/cm^2 C
$_{82}$Pb	206(99.1)	0.90	Evaporated	0.02 mg/cm^2 C
	208(99.3)	0.23	Evaporated	0.02 mg/cm^2 C
$_{83}$Bi (nat)	209(100)	0.36	Evaporated	0.2 mg/cm^2 Al
$_{90}$Th (nat)	232(100)	0.08	Evaporated	0.04 mg/cm^2 C

[a]Atomic mass and percent composition.
[b]Estimated uncertainty $\pm 15\%$.
[c]Supplied by MicroMatter Co., Eastsound, WA.

III. DATA

A. Angular correlations and angular distributions

Angular correlations were obtained at one or more angles for most of the heavier targets $A > 180$. Several of these, taken at large target-detector distances (30 cm) to minimize errors in $\theta_1 - \theta_2$, are shown in Fig. 1. Also shown are the angles expected for full momentum transfer to the compound system (^{3}He + target) yielding the observed fission-fragment kinetic energies. The latter correspond to $E^* = 30$ to 60 MeV in the compound system. In general the observed maxima are close to those expected for full momentum transfer and, if anything, may be shifted slightly *forward* (0.5° to 1°) from this angle. Such a shift would imply extra emitted momentum (e.g., due to ejected particles) in the backward direction with respect to the recoiling compound system.

Particularly with heavy projectiles, one often observes shifts in the angular correlations back from full momentum transfer.[19] This is attributed to processes which carry off momentum in the forward direction, e.g., incomplete fusion or direct reactions. These processes do not appear to be as important for low energy ^{3}He-induced fission.

A similar effect, viz., angular correlations shifted slightly forward from complete momentum transfer, may be present in data for ^{6}Li projectiles.[20] Also, anomalies have been reported in the back-angle spectrum of fast neutrons produced in the (^{3}He, xn) reaction.[21] Since both ^{3}He and ^{6}Li are weakly bound, strongly absorbed projectiles similar fission mechanisms may be involved, e.g., fission primarily induced by head-on collisions (rather than peripheral

FIG. 2. Angular distributions, $E(^3\text{He}) = 44.5$ MeV, for coincident fission fragments. The curves are least-squares fits to the data using $\sigma_F(\theta) = \sigma_0(1 + C\cos^2\theta)$ with the following values of C: Th, $C = 0.53$; Bi, $C = 0.73$; Au, $C = 1.29$; Re, $C = 1.60$; Ta, $C = 1.4$.

collisions) with fast particles ejected backwards. Data at higher ^{3}He and/or ^{6}Li bombarding energies would help clarify this.

Angular distributions were obtained for most of the heavier targets (Fig. 2). The cross sections were obtained from measurements of noncoincident fission fragments, or by integration of the angular correlations to obtain the equivalent information. Also, the absolute cross sections for ^{232}Th and ^{197}Au at $E(^3\text{He}) = 44.5$ MeV were checked using plastic fission-fragment track detectors and were found to agree with the detector data within the known uncertainties. Although the $\sigma_F(\theta)$ exhibit a slight anisotropy[2,3] they are primarily indicative of a statistical-type fission-decay process from the compound system[3] and are well described by the form

$$\sigma_F(\theta) = \sigma_0(1 + C\cos^2\theta) .$$

The quantity C, here typically ≈ 0.1 [for Th, $E(^3\text{He}) = 19.1$ MeV] to ≈ 1.3 [for Au, $E(^3\text{He}) = 44.5$ MeV] describes the $\theta = 0°$ to $\theta = 90°$ asymmetry and is related to the angular momentum of the fissioning compound system ($\leq 25\hbar$).[2,3]

B. Total cross sections

Total fission cross sections σ_F were obtained from integration of $\sigma_F(\theta)$, where measured, or from $\sigma_F(\theta)$ at the angles available and interpolation. The fissilities deduced, σ_F/σ_T, where σ_T is a calculated total reaction cross section (see Sec. IV), are presented in Fig. 3 as a function of
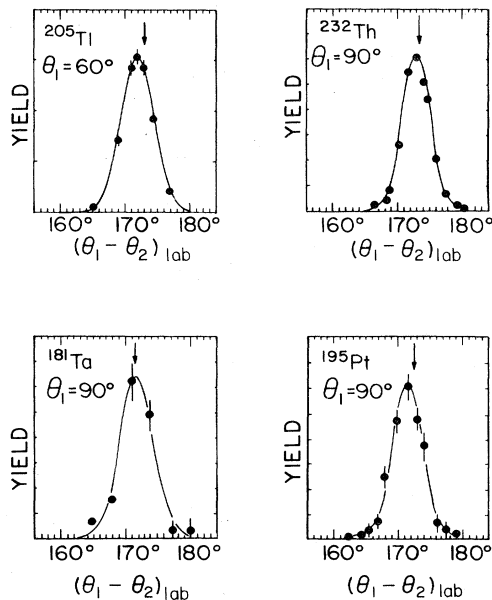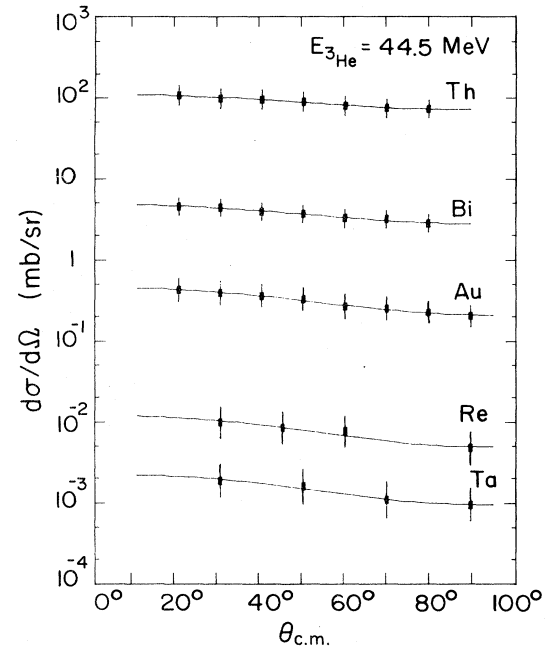
FIG. 1. Angular correlations deduced between coincident fission fragments. The arrows indicate the predicted position for binary fission with full momentum transfer from the ^{3}He projectile to the compound nucleus with the latter at $E^* \approx 55$ MeV. The angular acceptance of the detectors was $\leq 2.9°$ (full width).
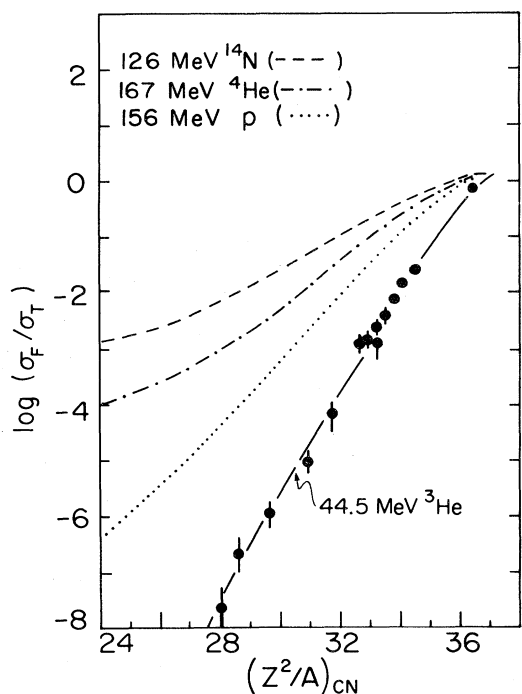
FIG. 3. Fissilities deduced in this work (44.5 MeV incident ^{3}He) compared with other data (Refs. 7, 10, and 27).

FIG. 4. Total kinetic-energy release (corrected for post-fission neutron emission) as a function of $Z^2/A^{1/3}$ for the ^{3}He + target system, $E(^3$He$)=44.5$ MeV. The solid curve is a calculation using the semiempirical relation determined by Viola (Ref. 24) while the broken curve is a theoretical calculation due to Nix (Ref. 23). We have assumed $\langle E_{K,\text{tot}} \rangle = 185 \pm 1$ MeV for ^{252}Cf (Ref. 22).

$(Z^2/A)_{\text{CN}}$, the Z^2/A of the ^{3}He + target compound nucleus, and compared with other data. Below $A=210$, σ_F falls off exponentially with the fissility parameter (Z^2/A), as expected,[2,3] with

$$\log_{10}\sigma_F \text{ (mb)} = 0.85(Z^2/A)_{\text{CN}} - 27.4$$

for   (1)

$$27 < (Z^2/A)_{\text{CN}} < 34 \ .$$

It is apparent in Fig. 3 that increased bombarding energy and/or projectile mass (i.e., incident angular momentum) has a large effect on the measured fissilities. Generalized fissility formulae[14] are obviously not applicable.

Superimposed on the smooth variation of σ_F and σ_F/σ_T with $(Z^2/A)_{\text{CN}}$ is some structure, particularly near the doubly magic nucleus ^{208}Pb. We attribute this to variations in the nuclear level densities near closed shells which affect the competition between fission and nucleon emission.[2,3]

C. Kinetic energy release

The observed fission-fragment kinetic energies for $E(^3$He$)=44.5$ MeV have been adjusted for pulse-height defects in the detectors[22] and energy losses in the target material and backing. The observed post-fission fragment total kinetic energies $\langle E_{K,\text{tot}} \rangle_{\text{obs}}$ have then been corrected for neutron emission using an estimated value for the average number of post-fission neutrons emitted, $\bar{\nu}(\approx E^*/12)$, and the relation[23,24]

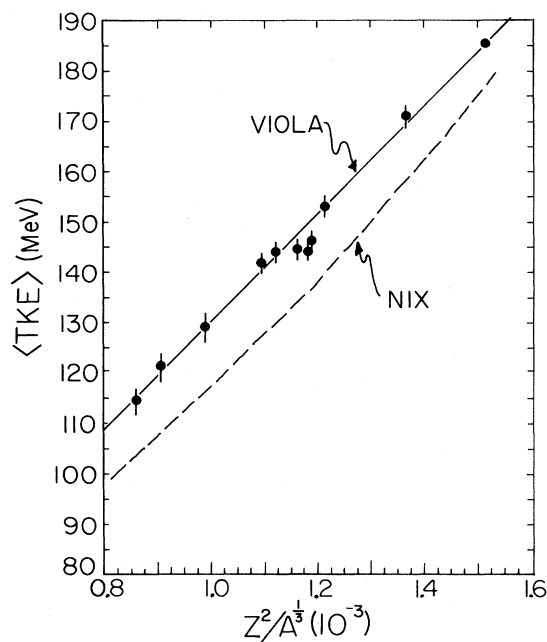$$\langle E_{K,\text{tot}} \rangle = \langle E_{K,\text{tot}} \rangle_{\text{obs}} \left[1 + \frac{\bar{\nu}}{2A} \left[\frac{A_1}{A_2} + \frac{A_2}{A_1} \right] \right] \tag{2}$$

to give, for symmetric fission,

$$\langle E_{K,\text{tot}} \rangle = \langle E_{K,\text{tot}} \rangle_{\text{obs}}[1 + E^*/(12A)] \ , \tag{3}$$

where E^* is the calculated excitation energy of the fissioning system ($E^* \approx 55$ MeV). The most probable total kinetic energies, $\langle E_{K,\text{tot}} \rangle$, are shown in Fig. 4 versus the Coulomb energy parameter $(Z^2/A^{1/3})_{\text{CN}}$.

The present results follow closely those observed with other ions, $\langle E_{K,\text{tot}} \rangle \propto Z^2/A^{1/3}$, and, in particular, the semiempirical relation determined by Viola,[24]

$$\langle E_{K,\text{tot}} \rangle = 0.1071(Z^2/A^{1/3})_{\text{CN}} + 22.2 \text{ MeV} \ . \tag{4}$$

Differences of a few MeV between the ^{3}He $\langle E_{k,\text{tot}} \rangle$ data and those obtained using heavy ions[19,23,24] are expected due to differences in the excitation energies and angular momenta (and hence rotational energy) of the fissioning compound systems.[25] No evidence for these differences is apparent, although a slightly lower $\langle E_{K,\text{tot}} \rangle$ is indicated (Fig. 4) near the doubly magic nucleus ^{208}Pb.

D. Mass distributions

Relative mass distributions have been inferred using the relation[2,3]

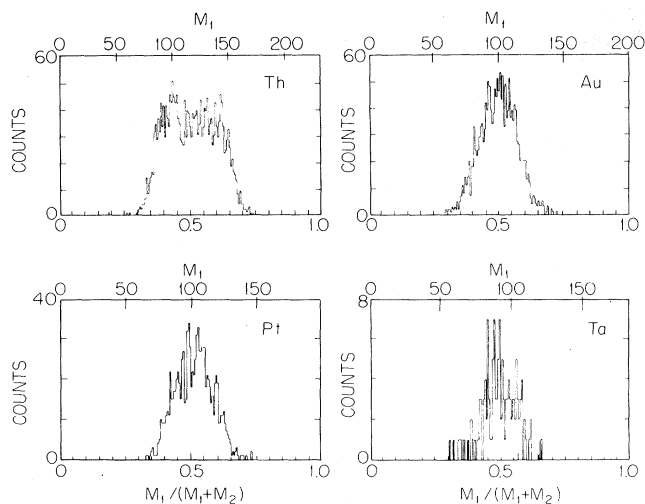FIG. 5. Relative fission-fragment mass spectra, assuming $M_1/(M_1+M_2) \simeq E_2/(E_1+E_2)$ and $M_1+M_2 \simeq A_{tgt}+3$. The spectra correspond to correlation angles near the maxima (Fig. 1) with $\theta_1 \approx 90°$.

$$\frac{M_1}{M_1+M_2} \approx \frac{E_2}{E_1+E_2}, \qquad (5)$$

where E_1 and E_2 are the coincident-fragment kinetic energies, corrected for detector pulse-height defects and energy losses in the target material. Some of these distributions are shown in Fig. 5. Owing to energy losses in the targets and backings, and uncertainties in the relative energy calibrations, the $M_1/(M_1+M_2)$ scales have an uncertainty of ± 0.1. The absolute mass scales assume

$$M_1+M_2 = A_{CN} \approx A_T+3 ,$$

and also are only approximate due to prefission particle evaporation. The latter is calculated to be ≤ 4 nucleons for elements $A < 210$. [The flight paths used here were too short to give good mass resolution for heavy fragments, i.e., $< \pm 10$ u. The time-of-flight (TOF) information was used primarily for pileup and background suppression of lighter ions, viz., $A < 20$.]

The relative mass distributions for $A \leq 210$ appear to be symmetric (Fig. 5). The widths (FWHM) of the fission-fragment mass distributions are 15 to 30 u (15 to 30%) and tend to increase (fractionally) for decreasing $(Z^2/A)_{CN}$, indicating perhaps the transition to more asymmetric fission near the $A=140$ mass region.[26,27]

IV. ANALYSIS

A. Theory

We have performed fission calculations[28] using a modified version of the code ALICE (Ref. 29) which includes provisions for precompound nucleon emission via a geometry-dependent hybrid model.[30] The fission is treated as a statistical decay process of the final compound nu-

cleus using the Bohr-Wheeler theory as applied by Cohen, Plasil, and Swiatecki.[28]

Calculations were done with either the parabolic-model approximation or the optical model for the entrance-channel ³He transmission coefficients and total reaction, i.e., CN cross sections (σ_T). Optical-model transmission coefficients were utilized for the proton-, neutron-, and alpha-decay channels. LDM masses without pairing energies were used to calculate binding energies and fission barriers.

The crucial parameters which enter into statistical-fission theory are the nuclear level densities (a_N), the level density at the fission saddle point (a_F), and the fission barrier B_F. The latter is usually referenced to the LDM fission barrier B_F^{LDM}. One expects $A/10 < a_N < A/7$, and $a_F/a_N = 1.00$ to 1.20. An extensive analysis[31] of α-induced fission excitation functions (which are quite sensitive to a_F/a_N) indicates $a_F/a_N \approx 1.08$ with $a_N = A/9 \pm 1$ for $A \approx 200$. Bishop et al.[32] calculate the dependence of a_F/a_N on the relative deformation at the fission saddle point and suggest that a_F/a_N should approach unity in lighter nuclei $(A < 200)$ with $a_F/a_N \approx 1.02$ typical for $A \approx 200$. As mentioned in the Introduction, some analyses of heavy-ion and high-energy nucleon-induced fission indicate $B_F \approx 0.6$ to 0.7 B_F^{LDM}, for $a_F/a_N = 1.0$ to 1.10, or, alternately, $B_F \approx B_F^{LDM}$ with $a_F/a_N \geq 1.20$, where, however, B_F is the barrier at *large* angular momentum.

B. Fission barriers, E(³He=44.5 MeV)

Calculations for E(³He)=44.5 MeV were initially done with[33] $B_F = B_F^{LDM}$ and a range of a_F/a_N values with $a_N = A/8$. Then a_F/a_N was fixed (=1.0) and B_F varied. The dependence of σ_F on these parameters is shown in Fig. 6 (the dependence on the absolute value of a_N or a_F is relatively weak). Inclusion of precompound nucleon emission reduces σ_F by about 50% at E(³He)=44.5 MeV, but
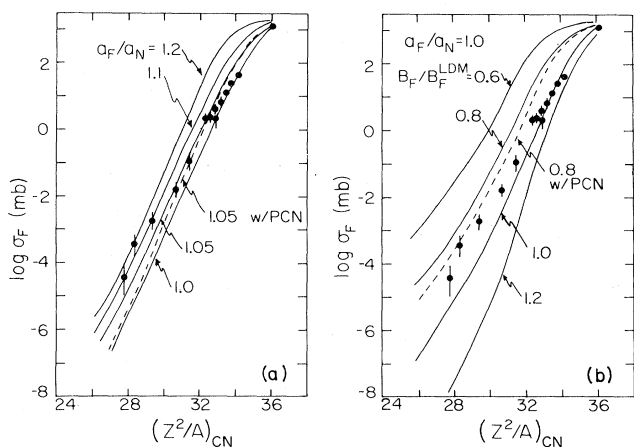

FIG. 6. A comparison of fission data with statistical-model calculations (a) as a function of the ratio of level density parameters, a_F/a_N, for $B_F = B_F^{LDM}$, and (b) as a function of the fission barrier B_F, for $a_F/a_N = 1.0$ (precompound nucleon emission not included unless otherwise noted). Z^2/A_{CN} refers to the compound system ³He + target.
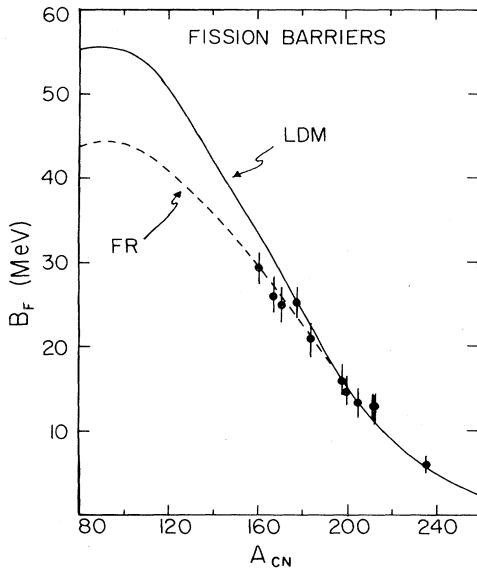
FIG. 7. Statistical-model fission barriers obtained in analysis of the present data (with $a_F/a_N = 1.05$) compared with LDM values (Ref. 1) and values calculated with a finite-range nuclear force (Ref. 34).

otherwise the variations with a_F/a_N and B_F are similar to those shown in Fig. 6. (Subsequent calculations included precompound nucleon emission.)

In general, the experimental σ_F values decrease less rapidly with $(Z^2/A)_{CN}$ than predicted using $B_F = B_F^{LDM}$ and a fixed value for a_F/a_N. In order to fit the observed behavior, a_F/a_N would need to be increased 5–10 % for decreasing mass, or, alternately, B_F decreased slightly (10–20 %) relative to B_F^{LDM}. The former seems unlikely,[32] except near the closed shells at $A = 208$ or $A = 132$ where a_N may be decreased slightly, and hence a_F/a_N increased.[3,32] We thus attribute the increase in σ_F to a slight reduction in B_F relative to B_F^{LDM} for $A < 200$.

The exact values of B_F required depend on the value of a_F/a_N assumed for $A < 200$. (The data $A \cong 208$ will be treated in IV C.) If we take $a_F/a_N \approx 1.05$ for this mass region as suggested by analyses of excitation functions (Sec. IV D and Ref. 31) and adjust B_F to produce agreement with the data (including precompound nucleon emission in the calculations) we obtain the fission barriers shown in Fig. 7, namely, $B_F \approx B_F^{LDM}$ at $A \approx 200$ and $B_F \approx 0.9B_F^{LDM}$ at $A \approx 160$ [$(Z^2/A)_{CN} \approx 28$]. Also shown in Fig. 7 are results of barrier calculations of Nix, Krappe, and Sierk[34,35] using a folding model.

Although $B_F \approx 0.9B_F^{LDM}$ for $A \approx 160$, values of $B_F < 0.8B_F^{LDM}$ appear to be excluded by the data at $E(^3He) = 44.5$ MeV for reasonable choices of a_F/a_N. The low fission and fusion barriers reported for heavy ions appear to be related to problems in extrapolating fission barriers deduced at high angular momenta to $l \cong 0\hbar$.[13,34−36] Recent reanalyses[37] of heavy-ion induced fission and an analysis of ^{6}Li-induced fission[38] also appear to be con-

sistent, $B_F \cong B_F^{LDM}$ $(l = 0\hbar)$, and exclude values of $B_F \lesssim 0.6B_F^{LDM}$ $(l = 0\hbar)$ for $A < 210$.

C. The region near $A = 208$

The region near doubly magic $A = 208$ [$(Z^2/A)_{CN} \approx 33$] exhibits an increase in σ_F relative to the smooth trend above and below this mass region. This increase can be reproduced by increasing a_F/a_N (or decreasing a_N) by about 5 to 8% in this region. This is comparable with the effect seen in other fission measurements.[2,3] The best fit to σ_F near $A = 208$ also would require $B_F \approx 1.1B_F^{LDM}$ but shell effects[3] in B_F are dominant in this mass region, since B_F^{LDM} is only a few MeV.

D. Excitation functions

Fission excitation functions, with complete or partial angular distributions, and angular correlations were measured for Th, Bi, Au, and Ta targets (Table I) for $E(^3He) = 19.1$ to 44.5 MeV. The total fission cross sections deduced are shown in Fig. 8 together with calculations using standard parameter sets (parabolic-model approximation). Again, one does not require $B_F \ll B_F^{LDM}$ to reproduce the general features of the data although Ta is best fit with $B_F \approx 0.8B_F^{LDM}$ $(a_F/a_N = 1.0)$ or $B_F \approx 0.9B_F^{LDM}$ $(a_F/a_N = 1.05)$. Use of finite-range fission barriers[34−36] or adding a constant barrier decrement[13] does not substantially improve the fits to the excitation functions since unlike heavy ions[13] our data span a small range in angular momentum ($l \cong 5\hbar$ to $20\hbar$).
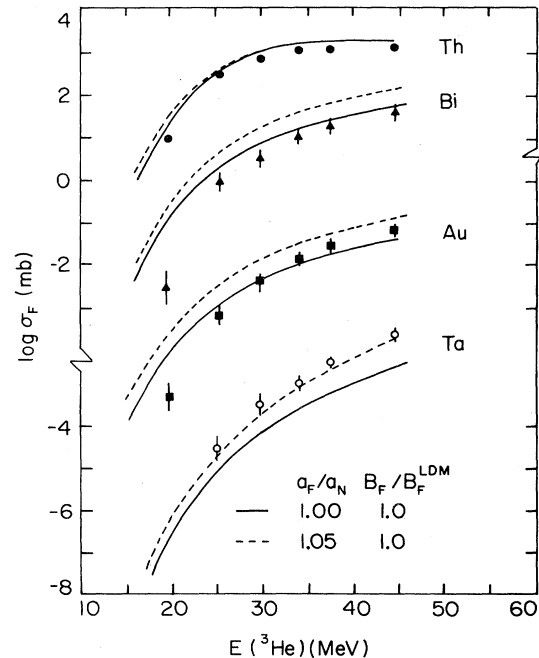

FIG. 8. Fission excitation functions compared with statistical-model calculations for the parameters shown. The calculations include precompound nucleon emission and employ the parabolic-barrier approximation for the incident ^{3}He channel (see text).

Low values for a_F/a_N (≈ 1.0) do not yield fits to the shapes of the excitation functions as well as values of $a_F/a_N = 1.05$ to 1.10 ($B_F \geq B_F^{LDM}$). This has also been observed with α-induced fission[31] although inclusion of precompound nucleon emission, which is important above $E(\text{He}) \approx 30$ MeV, reduces this effect. Calculations using the optical model with suitable parameters[39] for the ³He-nucleus interaction yield σ_F values equal to or greater than the values shown in Fig. 8 and for example would require $B_F \geq B_F^{LDM}$ to fit most of the data. Thus although the ³He-nucleus potential can affect the magnitude and shape of the fission excitation functions, particularly at lower bombarding energies, drastic reductions in B_F relative to B_F^{LDM} are not required.

V. CONCLUSIONS

Analysis of 19.1 to 44.5 MeV ³He-induced fission of targets $A = 159$ to $A = 232$ does not appear to require sub-stantially reduced fission barriers relative to liquid-drop-model values, in contrast to some analyses of heavy-ion and high-energy light-ion data. The data are compatible with $B_F = 0.8 B_F^{LDM}$ to 1.1 B_F^{LDM} with $a_F/a_N = 1.0$ to 1.05, respectively. The angular correlations are consistent with complete or perhaps slightly greater than complete momentum transfer to the compound system.

[1]W. D. Myers and W. J. Swiatecki, Nucl. Phys. 81, 1 (1966).

[2]E. K. Hyde, *The Nuclear Properties of the Heavy Elements* (Dover, New York, 1971), Vol. 3.

[3]R. Vandenbosch and John R. Huizenga, *Nuclear Fission* (Academic, New York, 1973).

[4]F. D. Becchetti, in the Proceedings of the International Conference on Nuclear Physics, Berkeley, 1980, LBL Report No. LBL-11118, 1980, p. 285.

[5]F. L. Milder, J. Jänecke, and F. D. Becchetti, Nucl. Phys. A276, 72 (1977); J. Jänecke, F. D. Becchetti, and D. Overway, *ibid.* A343, 161 (1980).

[6]T. Sikkeland *et al.*, Phys. Rev. 135, B669 (1964); Phys. Rev. C 3, 329 (1971).

[7]B. Borderie, F. Hanappe, C. Ngô, J. Péter, and B. Tamain, Nucl. Phys. A220, 93 (1974); C. Cabot, C. Ngô, J. Péter, and B. Tamain, *ibid.* A244, 134 (1975).

[8]M. Beckerman and M. Blann, Phys. Rev. C 17, 1615 (1978).

[9]F. Plasil *et al.*, Phys. Rev. Lett. 45, 333 (1980).

[10]B. D. Pate and J. Péter, Nucl. Phys. A173, 520 (1971).

[11]L. A. Vaishnene, L. N. Andronenko, G. G. Kovehevny, A. A. Kotov, and W. Neubert, Z. Phys. A 302, 143 (1981).

[12]G. Andersson *et al.*, Z. Phys. A 293, 241 (1979).

[13]M. Blann and T. A. Komoto, Phys. Rev. C 26, 472 (1982).

[14]J. R. Nix and E. Sassi, Nucl. Phys. 81, 61 (1966).

[15]J. R. Huizenga, R. Chaudry, and R. Vandenbosch, Phys. Rev. 126, 210 (1962); E. F. Neuzil, J. Inorg. Nucl. Chem. 38, 2153 (1976), and references cited therein; R. M. Williams, R. D. Kieburtz, and E. F. Neuzil, *ibid.* 35, 3651 (1973).

[16]Grant M. Raisbeck and J. W. Cobble, Phys. Rev. 153, 1270 (1967).

[17]H. C. Britt, H. E. Wegner, and J. C. Gursky, Phys. Rev. 129, 2239 (1963); A. Khodai-Joopari, University of California Report No. UCRL-16489, 1966 (unpublished); F. S. Plasil, D. S. Burnett, H. C. Britt, and S. G. Thompson, Phys. Rev. 142, 696 (1966).

[18]K. G. Kuvatov *et al.*, Yad. Fiz. 14, 79 (1971) [Sov. J. Nucl. Phys. 14, 45 (1972)]; A. V. Ignatyuk *et al.*, Yad. Fiz. 21, 1185 (1975) [Sov. J. Nucl. Phys. 21, 612 (1976)].

[19]V. E. Viola, Jr., *et al.*, Nucl. Phys. A174, 321 (1971); Phys.

Rev. C 26, 178 (1982); E. Duek *et al.*, Z. Phys. A 307, 221 (1982); 307, 237 (1982); F. Saint Laurent *et al.*, Phys. Lett. 110B, 372 (1982).

[20]H. Freiesleben, G. T. Rizzo, and J. R. Huizenga, Phys. Rev. C 12, 42 (1975).

[21]C. A. Fields, F. W. N. DeBoer, R. A. Ristinen, and E. Sugarbaker, Phys. Lett. 114B, 81 (1982).

[22]S. B. Kaufman *et al.*, Nucl. Instrum. Methods 115, 47 (1974); H. Henschel *et al.*, *ibid.* 190, 125 (1981).

[23]J. R. Nix, Nucl. Phys. A130, 241 (1969).

[24]V. E. Viola, Jr., Nucl. Data A1, 391 (1966).

[25]J. P. Unik, J. G. Cuninghame, and I. F. Croall, in *Physics and Chemistry of Fission* (IAEA, Vienna, 1969), p. 717.

[26]H.-Å. Gustafsson *et al.*, Phys. Rev. C 24, 769 (1981).

[27]F. D. Becchetti *et al.*, Phys. Rev. C 28, 276 (1983); M. Maurette and C. Stephan, in *Physics and Chemistry of Fission* (IAEA, Vienna, 1965), Vol. 2, p. 307; O. E. Shigaev *et al.*, Yad. Fiz. 35, 567 (1982) [Sov. J. Nucl. Phys. 35, 328 (1982)].

[28]S. Cohen, F. Plasil, and W. J. Swiatecki, Ann. Phys. (N.Y.) 82, 557 (1974).

[29]M. Blann, Program ALICE, University of Rochester Report No. UR-NSRL-181 (unpublished).

[30]M. Blann, Annu. Rev. Nucl. Sci. 25, 123 (1975).

[31]L. G. Moretto, S. G. Thompson, J. Routti, and R. C. Gatti, Phys. Lett. 38B, 471 (1972).

[32]C. J. Bishop, I. Halpern, R. W. Shaw, Jr., and R. Vandenbosch, Nucl. Phys. A198, 161 (1972).

[33]W. D. Meyers and W. J. Swiatecki, Ark. Fys. 36, 343 (1967).

[34]H. J. Krappe, J. R. Nix, and A. J. Sierk, Phys. Rev. C 20, 992 (1979).

[35]P. Möller and J. R. Nix, Nucl. Phys. A272, 502 (1976).

[36]M. G. Mustafa, P. A. Baisden, and H. Chandra, Phys. Rev. C 25, 2524 (1982).

[37]F. Plasil *et al.*, Phys. Rev. Lett. 45, 333 (1980); M. Blann, *ibid.* 49, 505 (1982); F. Plasil, *ibid.* 49, 506 (1982).

[38]S. E. Vigdor *et al.*, Phys. Rev. C 26, 1035 (1982).

[39]C. M. Perey and F. G. Perey, At. Data Nucl. Data Tables 17, 1 (1976), and references cited therein.